Available online at www.sciencedirect.com
SCIENCE DIRECT®
ELSEVIER
Simulation Modelling Practice and Theory 12 (2004) 129–146
SIMULATION MODELLING PRACTICE AND THEORY
www.elsevier.com/locate/simpat

Heart sound analysis for symptom detection and computer-aided diagnosis

Todd R. Reed [a,*], Nancy E. Reed [a], Peter Fritzson [b]

[a] *Department of Electrical Engineering, University of Hawaii, 2540 Dole Street, Honolulu, HI 96822, USA*

[b] *Department of Computer and Information Science, Linköping University, Sweden*

Received 26 August 2002; received in revised form 5 September 2003; accepted 24 November 2003

Abstract

Heart auscultation (the interpretation by a physician of heart sounds) is a fundamental component of cardiac diagnosis. It is, however, a difficult skill to acquire. In this work, we develop a simple model for the production of heart sounds, and demonstrate its utility in identifying features useful in diagnosis. We then present a prototype system intended to aid in heart sound analysis. Based on a wavelet decomposition of the sounds and a neural network-based classifier, heart sounds are associated with likely underlying pathologies. Preliminary results promise a system that is both accurate and robust, while remaining simple enough to be implemented at low cost.

Keywords: Auscultation; Cardiac; Diagnosis; Frequency analysis; Heart; Linear model; Sound analysis; Phonocardiogram

1. Introduction

Heart auscultation (the monitoring of sounds produced by the heart and blood circulation) is a fundamental tool in the diagnosis of heart disease. While somewhat eclipsed in the research literature due to the advent of electrocardiographic (ECG) and echocardiographic methods, there are heart defects that are difficult to detect using ECG (e.g., structural abnormalities in natural or implanted heart

* Corresponding author. Tel.: +1-808-956-5309.
E-mail addresses: trreed@hawaii.edu (T.R. Reed), nreed@hawaii.edu (N.E. Reed), petfr@ida.liu.se (P. Fritzson).

1569-190X/$ - see front matter
doi:10.1016/j.simpat.2003.11.005

valves, and defects characterized by heart murmurs and abnormal sounds). Furthermore, auscultation remains the primary tool for screening and diagnosis in primary health care, due in part to the higher cost and relatively limited availability of the equipment, and to the special skills necessary to administer and interpret the results of ECG and echocardiography. In some circumstances, particularly in remote areas or developing countries, auscultation may be the only means available.

However, forming a diagnosis based on sounds heard through either a conventional acoustic or an electronic stethoscope is itself a very special skill, one that can take years to acquire. Because this skill is also very difficult to teach in a structured way, the majority of internal medicine and cardiology programs offer little or no such instruction. Despite its obvious utility, primary care physicians are documented to have poor auscultatory skills [1–3]. It would be very useful if the benefits of auscultation could be obtained with a reduced learning curve, using equipment that is low-cost, robust, and easy to use.

The complex and highly nonstationary nature of heart sound signals can make them challenging to analyze in an automated way. However, recent technological developments have made extremely powerful digital signal-processing techniques both widely accessible and practical. Local frequency analysis and wavelet (local scale analysis) approaches are particularly applicable to problems of this type. Some of these methods have been applied to study the fundamental mechanisms underlying the production of sound by the heart, and the correlation between these sounds and various heart defects (e.g., [4–13]). For an excellent survey and discussion of work in this area see [14].

Despite the clear success of digital signal-processing (DSP) based techniques, many heart sounds associated with defects remain subtle, and difficult to detect and discriminate from similar sounds with no underlying pathology.

Some of the same technological advances that have supported DSP oriented methods have also facilitated the development of increasingly sophisticated models of the heart, from relatively simple models focusing on sound formation such as [15], to full 3-D structural models.

The goal of this work is to combine local analysis methods, information provided via modeling, and classification techniques to detect, characterize and interpret sounds corresponding to symptoms and signs important for cardiac diagnosis. It is hoped that the results of this analysis may prove valuable in themselves as a diagnostic aid, and as input to machine diagnostic systems, as for example the Fallot computational model [16]. The modeling and analysis techniques described are general and could be applied to a broad range of signal-processing problems.

2. The structure of heart sounds

Heart sounds are complex and highly nonstationary signals. The "beats" associated with these sounds are reflected in the signal by periods of relatively high activity, alternating with comparatively long intervals of low activity.

The cardiac cycle consists of two periods, systole and diastole [17]. Four classes of sound components may be audible on heart auscultation: the primary components (S_1, S_2, S_3, and S_4) are short "beats", the other classes of sounds are murmurs (longer duration), clicks, and snaps. S_1 and S_2 are always audible in a normal patient. S_4, clicks, snaps, and organic murmurs (as opposed to "innocent" murmurs), are present only under abnormal circumstances, as described in more detail below.

A normal heart sound signal is shown in Fig. 1, with the two major components, S_1 and S_2, extracted and shown on expanded time axes at the bottom of the figure. The start of a heart cycle, systole, corresponds to the QRS complex on the ECG. S_1 occurs at the end of the isometric contraction period during systole, and S_2 occurs after the isovolumetric relaxation period during diastole. While the physiological origins of all the contributions to S_1 and S_2 are not agreed upon, it is clear that the closure of the mitral and tricuspid valves are major contributors to S_1. Similarly, the closure of the aortic and pulmonary valves are primary contributors to S_2 [18]. S_2 is composed of two components, A_2 and P_2 (corresponding to the aortic and pulmonary parts). Usually A_2 and P_2 are close together, but are just far enough apart that they can be heard as two "beats" within S_2. This is called a "split S_2". The width of the split in S_2 usually changes during inhalation and exhalation. If the two components cannot be distinguished, it is called a "single S_2". S_1 is usually single, but may be prominently split with some pathologies.

In addition to S_1 and S_2, third and fourth heart sounds (S_3 and S_4) may also be audible. When present, S_3 occurs shortly after S_2, and is associated with early diastolic filling of the ventricle. When S_4 is audible, it occurs shortly before S_1, and is

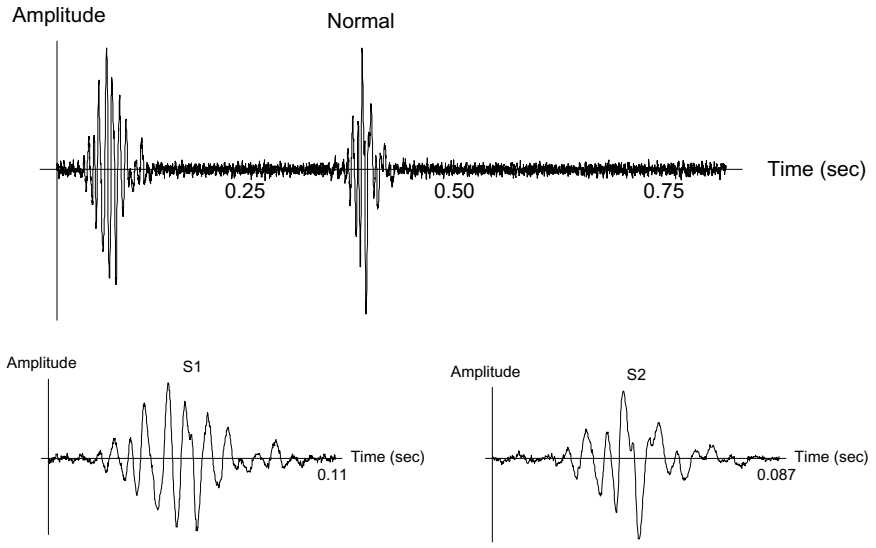

Fig. 1. A normal heartbeat (top), with S_1 and S_2 (bottom).

associated with late diastolic filling. An audible S_3 can be normal in the young (less than 35 years of age), while an audible S_4 is always considered abnormal.

The second class of sound components we describe are referred to as "murmurs". These may occur during either systole, diastole, or continue through both periods. Murmurs are caused by turbulence in blood flow or vibration of tissues. Murmurs may occur in normal hearts, where they are termed "innocent", or they may be caused by structural abnormalities, where they are termed "organic". Innocent murmurs are more frequently heard in children, and have been reported at rates of close to 90% [3].

The final classes of sound components are clicks and snaps. These sounds indicate abnormality, and are associated with valves opening. The most common click is a systolic ejection click, which occurs shortly after S_1 with the opening of the semilunar valves. The opening snap when present, occurs shortly after S_2 with the opening of the mitral and tricuspid valves. The mid-systolic click, as the term implies, usually occurs in mid-systole, with prolapse of the mitral valve. Clicks and snaps are distinctive features of some heart defects.

3. A simple heart sound model

The heart–thorax acoustic system, like the heart sounds themselves, is extremely complex. An approach to modeling complex systems that has proven useful in a number of domains is to approximate them as linear systems, and to use the tools developed for the study of such systems. Usually, this approach includes the assumption that the system of interest is time-invariant. Clearly, this is not the case here.

Durand and Pibarot [14] have proposed a linear model with both time-varying and time-invariant components. The system includes (in series) a subsystem which varies quickly with time (to represent the myocardial system), one which varies slowly with time (to model the respiratory system), and one which is time-invariant (to capture the behavior of the chest wall system). The model also includes impulse-like, stochastic, and periodic inputs to represent components of the heart sound due to events such as valve closure, stenotic and regurgitant murmurs, and musical murmurs, respectively.

The architecture of the model in [14] reflects the physiological structure of the heart–thorax system in a particularly elegant way. It provides an intuitive framework for understanding the dynamics of the system, and in situations where the implantation of intracardial transducers is feasible, provides a very good approach to system characterization.

The goal of this work, however, is to capture a diagnostically useful system description noninvasively. While the general approach described above is still valuable for this task, some approximations are required due to the lack of internal data. First of all, we will assume that the system is time-invariant during each of the resolvable heart sounds. This restriction is due to the fact that the responses to the events associated with each sound (e.g., the responses to the mitral and tricuspid valves closing in S_1) are generally not distinguishable at the chest wall. For the cur-

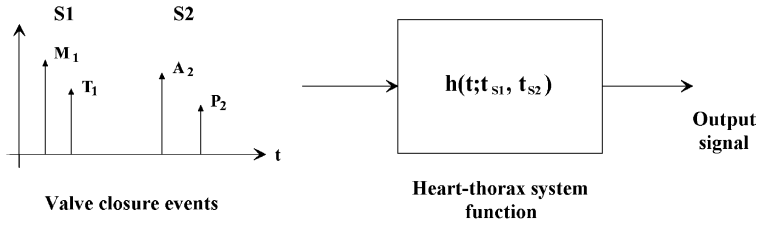

Fig. 2. A simple heart sound production model.

rent discussion, we will also restrict our model to the S_1 and S_2 heart sounds, assume that S_1 and S_2 are due only to the respective valve closings, and consider only cases which do not involve murmurs. These restrictions will be removed in Section 6, below.

The resulting simplified system is shown in Fig. 2. The input to the system, the valve closure events, are represented as impulses at the time of each event. The heart–thorax system is represented by its system function (impulse response). The notation $h(t; t_{S_1}, t_{S_2})$ indicates that the impulse response is time-varying, with different (time-invariant) responses over the periods of time corresponding to S_1 and S_2.

The characterization of the system, then, requires two steps. The first is the estimation of the relative amplitudes and times of the impulses representing the valve closures (a nontrivial task, given only the output signal). The second is the estimation of the S_1 and S_2 system functions. As is customary in linear systems, this second task will be done in the frequency domain, yielding the S_1 and S_2 transfer functions.

4. Determination of the inputs and transfer functions

To determine the relative locations and amplitudes of the input impulses, we first observe that for stable, damped linear systems, the response to an impulse is maximum in magnitude at the time corresponding to the application of the impulse. When the input to the system is a sequence of impulses, there will be peaks in energy in the output (which may or may not coexist with amplitude extrema in the output) for each impulse.

Locating such peaks is an ideal application for time–frequency or time-scale (wavelet) analysis. In these experiments, we have chosen (due to its relative symmetry and fast execution) to use a Coifman fourth order wavelet basis, decomposing the heart sounds into seven levels. The Lth level corresponds to a basis function of extent 2^L. The results of applying this decomposition to the normal heart sound from Fig. 1 (4096 samples in length, sampled at 8012 samples/s) are shown in Fig. 3. The A7 coefficients are the residual values after the last level of decomposition. The remaining coefficients belong to basis functions of the given length (e.g., the coefficients for decomposition level D5 are for basis functions $2^5 = 32$ samples long).

It is clear that the information content at the different levels varies widely. Making a compromise between signal-to-noise ratio and temporal resolution, we have chosen

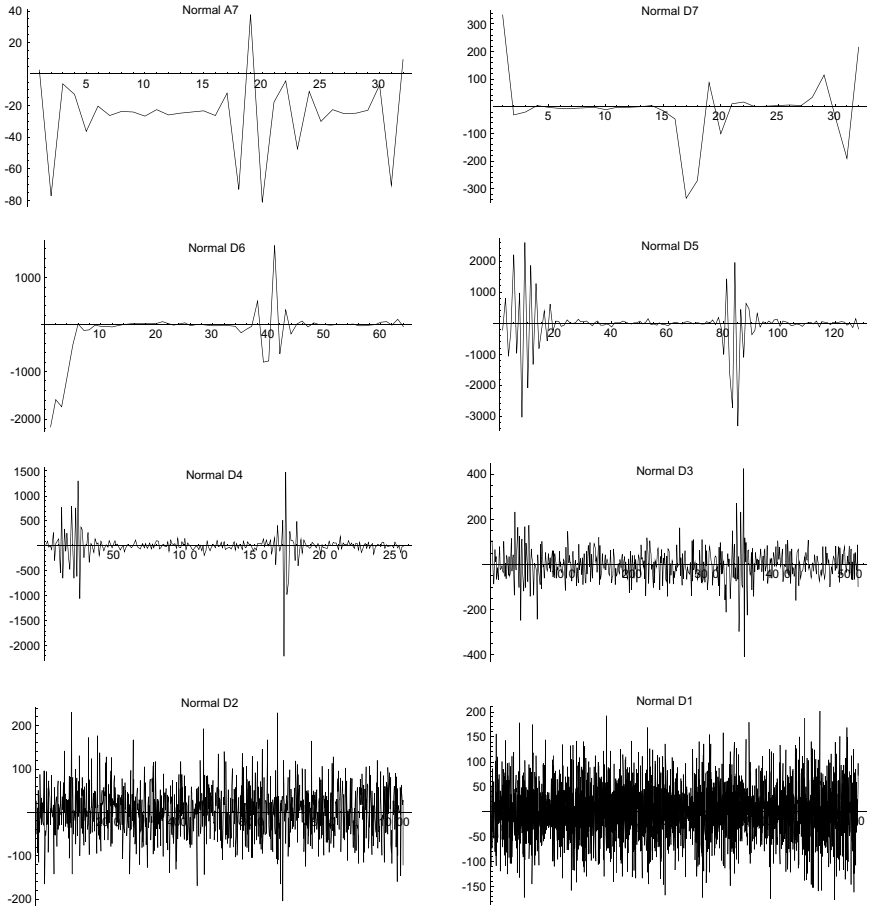

Fig. 3. The Coifman fourth order wavelet coefficients for a normal heartbeat.

to use the D5 coefficients to estimate the impulse locations. The result is a time resolution of 4 ms. This could be improved if a higher input signal-to-noise ratio could be obtained.

The magnitudes of the D5 coefficients for the normal heart sound are shown in Fig. 4, with the coefficients for the S_1 and S_2 sounds extracted and displayed on an expanded time-scale at the bottom of the figure. From these results, it is estimated that the input impulses occur at 18 and 30 ms in S_1 (with relative amplitudes of 0.665 and 0.917) and at 330 and 338 ms in S_2 (with relative amplitudes of 0.824 and 1.00). In normal subjects, the mitral and tricuspid, and aortic and pulmonary valves have generally been found to close within 10–30 ms of each other. The estimated time between closures for S_1 is therefore within the expected range, while that for S_2 is somewhat shorter.

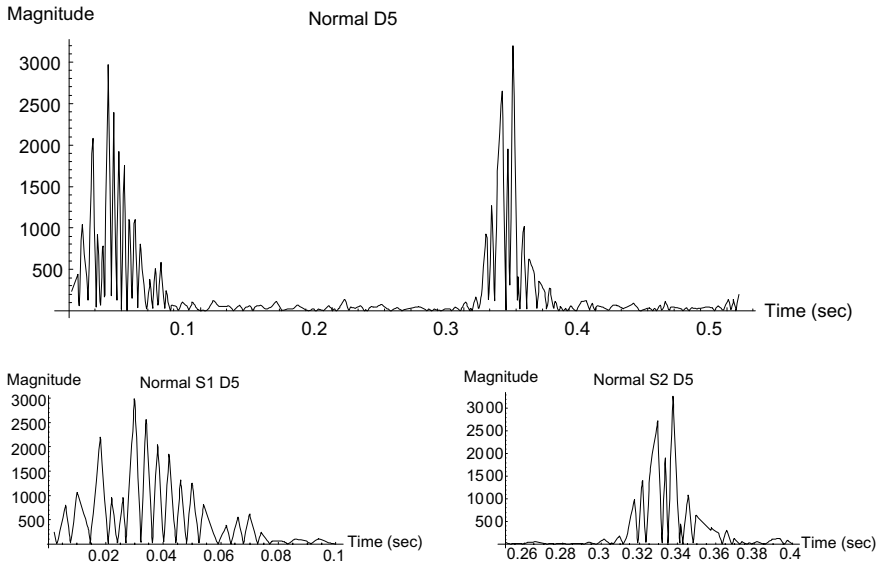

Fig. 4. The magnitude of the D5 wavelet coefficients for a normal heartbeat (top), and S_1 and S_2 (bottom).

With the input to the system established, the S_1 and S_2 transfer functions can be found by dividing the discrete Fourier transforms of the S_1 and S_2 heart sounds by the transforms of the impulse pairs generating the sounds. Note that this requires that the transforms of the impulse pairs not include nulls, a condition which is satisfied in this case. The resulting magnitude responses for the S_1 and S_2 transfer

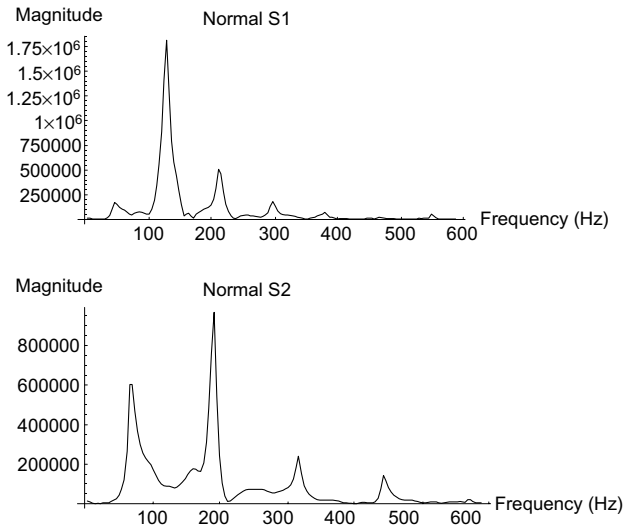

Fig. 5. The magnitude responses of the normal S_1 and S_2 transfer functions.

functions are shown in Fig. 5. Their utility in discriminating between normal and abnormal heart sounds will be demonstrated in the next section.

5. The characterization of abnormal heart sounds

We will consider two types of abnormal heart sounds in this section: those resulting from coarctation of the aorta, and those exhibiting so-called "splits."

5.1. Coarctation of the aorta

As an example demonstrating the value of the S_1 and S_2 transfer functions for diagnosis, we will consider the case of coarctation of the aorta. A heartbeat from a patient exhibiting this abnormality is shown in Fig. 6. While clearly different than the normal heartbeat in Fig. 1, the differences are difficult to quantify.

Coarctation of the aorta is a constriction of the aorta, restricting the flow of oxygenated blood from the left ventricle to the body. The result is elevated blood pressure in the left ventricle and the vessels before the coarctation, and reduced blood pressure in the circulatory system after the coarctation. Left ventricular hypertrophy (thickening of the walls of the left ventricle) results due to the increased pressure [17]. If left untreated, premature coronary artery disease is common, and may ultimately result in heart failure.

Following the procedure described above, the D5 level of the wavelet decomposition of the heartbeat was examined, and the times and amplitudes of the input impulses due to valve closure were estimated. The resulting impulses were at 14 and 26 ms for S_1 and 326 and 342 ms for S_2. Their relative amplitudes were 0.552, 1.0, 0.545 and 0.888, respectively. The S_1 and S_2 transfer functions were then computed,

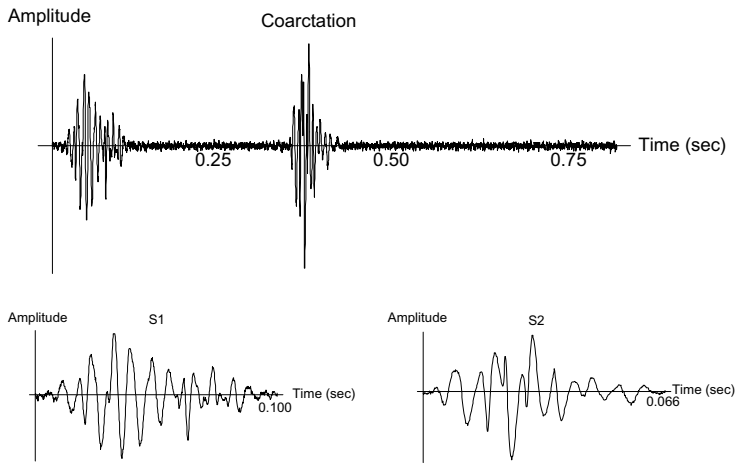

Fig. 6. A heartbeat resulting from coarctation of the aorta.

the magnitude plots of which are shown in Fig. 7.

Because this defect is associated with the aorta and left ventricle, it would be reasonable to expect its primary effects to be seen in S_2. Comparing the normal S_1 transfer function in Fig. 5 with the S_1 transfer function of the case with coarctation in Fig. 7, we see that they are in fact very similar.

Comparing the normal and abnormal S_2 transfer functions, however, there are clear differences. There are two pronounced additional peaks in the case with coarctation, together with shifts in the locations and relative amplitudes of the peaks observed in the normal case. Establishing a correlation between these effects and the underlying physiology will require substantial additional investigation.

Other defects often coexist with CA. A bicuspid aortic valve, for example is present in about 75% of CA cases. The presence of a bicuspid aortic valve usually means there is an accompanying aortic ejection click.

It would be natural at this point, given that the above discussions are in the frequency domain, to ask whether one could bypass the calculation of the S_1 and S_2 transfer functions and simply examine the S_1 and S_2 power spectra (avoiding the estimation of the valve closure times and amplitudes). The magnitudes of the Fourier transforms of S_1 and S_2 for these two cases are shown in Fig. 8. While sufficient study reveals that the basic features shown in the transfer functions exist in the Fourier transforms of the signals themselves (as they of course must), the distinguishing features between the cases are much more difficult to identify. Normalization by the Fourier transforms of the input impulse sequences, as done in the calculation of the transfer functions, serves to sharpen and enhance the features of interest.

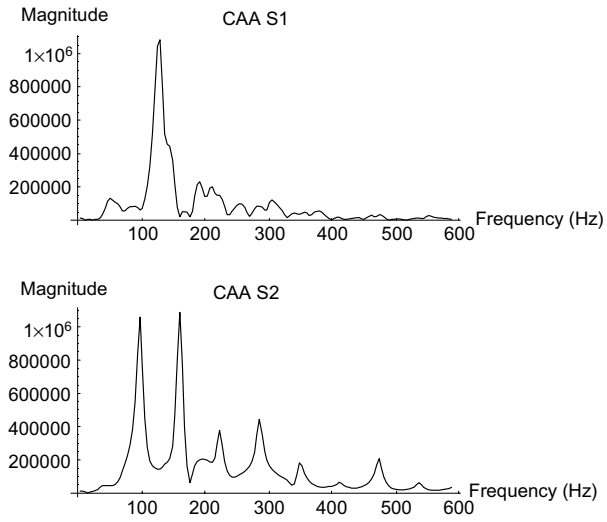

Fig. 7. The magnitude responses of the S_1 and S_2 transfer functions with coarctation of the aorta.

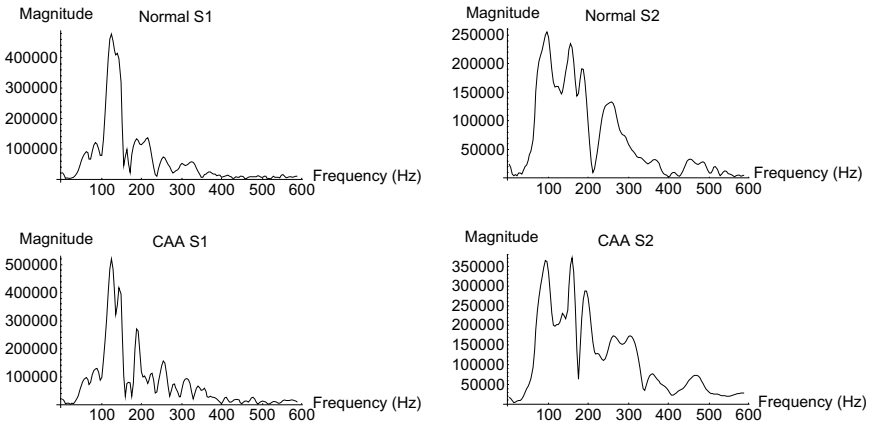

Fig. 8. The magnitudes of the Fourier transforms of the normal S_1 and S_2 sounds and those with coarctation of the aorta.

5.2. Split sounds

Because the mitral and tricuspid valves typically close within less than 30 ms, S_1 is usually perceived by physicians as a unified, single sound. That is, the components of the sounds due to the individual valve closures are not individually audible. S_2 is normally resolvable into two components (split), just at the threshold of audibility. The width of the split between A_2 and P_2 changes slightly with inhalation and exhalation. There are a number of circumstances that can lead to an abnormal splitting of S_2 (wide but normally moving, fixed splitting or reverse splitting) or an abnormal (split) S_1.

The time intervals between valve closures are therefore important diagnostic cues. Measured in milliseconds, the time intervals will be smaller with a faster heart rate and vice versa. As demonstrated above in the process of finding the S_1 and S_2 transfer functions, these time intervals can be estimated using local frequency/scale analysis.

A heart sound with an abnormally wide split S_2 is shown in Fig. 9. Examining the D5 wavelet coefficient magnitudes for this sound (Fig. 10), peaks can be seen at 14, 26, 338, and 382 ms. Based on these peaks, the interval between the closure of the mitral and tricuspid valves (in S_1) is estimated to be 12 ms, while the time between the closure of the aortic and pulmonary valves (in S_2) is estimated to be 44 ms. The interval between the closures in S_1 is therefore within the normal range, while the interval for S_2 is indicative of a wider than normal split.

6. A system for heart sound classification

A block diagram representing a simple system for heart sound classification is shown in Fig. 11. Heart sounds (sampled at an 8 kHz sample rate, 16 bits/sample) are first hand segmented into 4096 sample segments, each consisting of a single

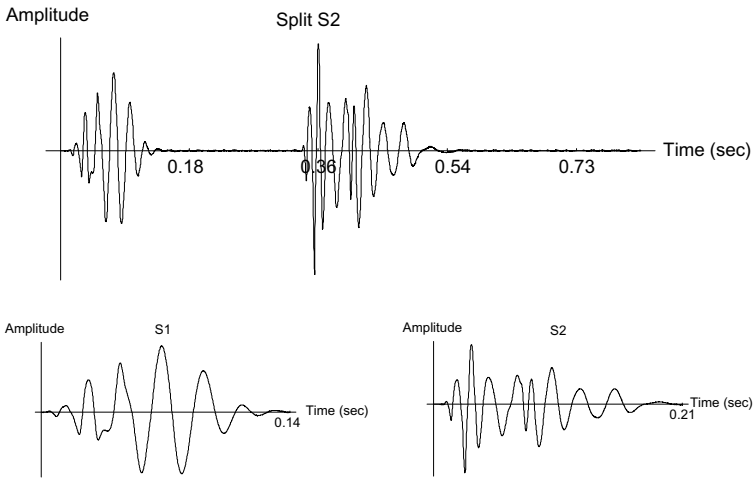

Fig. 9. A heartbeat with split S_2.

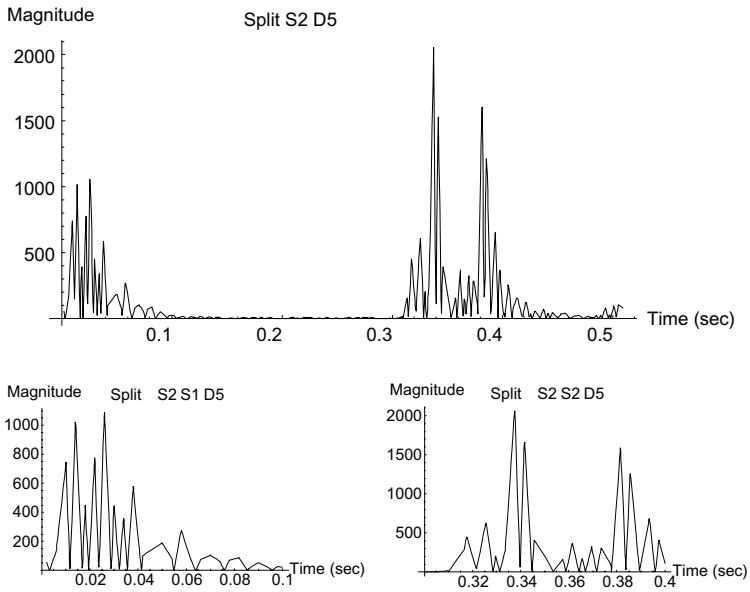

Fig. 10. The magnitude of the D5 wavelet coefficients for a heartbeat with split S_2 (top), and those for S_1 and S_2 (bottom).

heartbeat cycle. Each segment is transformed using a seven level wavelet decomposition, based on a Coifman fourth order wavelet kernel. The resulting transform vectors, 4096 values in length, are reduced to 256 element feature vectors by discarding

Fig. 11. A simple heart sound classification system.

the four levels with shortest scale. In addition to substantially simplifying the neural network in the classifier which follows, this step also reduces noise. The magnitudes of the remaining coefficients in each vector are calculated, then normalized by the vector's energy. Finally, each feature vector is classified using a three layer neural network (256 input nodes, 50 hidden nodes, and 5 output nodes).

7. Results and discussion

The system was evaluated using heart sounds corresponding to five different heart conditions: normal, mitral valve prolapse (MVP), coarctation of the aorta (CA), ventricular septal defect (VSD), and pulmonary stenosis (PS). CA often leads to an increased A_2 sound, while VSD often produces an increased P_2. In PS, the P_2 is soft and may not be audible, making S_2 appear single. A click may also be present.

The classifier was trained using 10 shifted versions (over a range of 100 samples) of a single heartbeat cycle from each type. Shifted training exemplars were used to provide a degree of shift invariance (since, as is well known, wavelet decompositions are generally not shift invariant). In this application, such shifts may occur due to variations in the heartbeat starting time, as found during the segmentation process.

The system was then presented heart sounds with varying degrees of additive noise for classification. Because the sample set available for this study was small, (one patient per heart condition, four heartbeat cycles per patient) the heartbeats used in generating the shifted training exemplars were also used as part of the basis for the evaluation set. Representative examples are shown in the left column of Fig. 12, with the effects of additive noise shown in the center and right columns. The feature vectors produced for these examples are shown in Fig. 13. Note that, while the effect of the additive noise can be seen in the feature vectors, key features remain relatively stable.

The resulting classification accuracy as a function of the added noise variance is shown in Fig. 14. For variances up to and including 3000 (corresponding to the signals and features in the third columns of Figs. 12 and 13), classification is 100% accurate for all heart sounds. Above a variance of 3000, the decrease in accuracy varies widely between the different sounds, from a fairly rapid decrease for the normal case to no decrease in the VSD case.

This can be explained in part by noting that, while the peak amplitudes of the normal components of each heart sound (the S_1 and S_2 components) are comparable in each case, the variance of the sounds differs widely (e.g., by a factor of approximately 16:1 comparing a typical normal heartbeat with one exhibiting VSD). Accounting

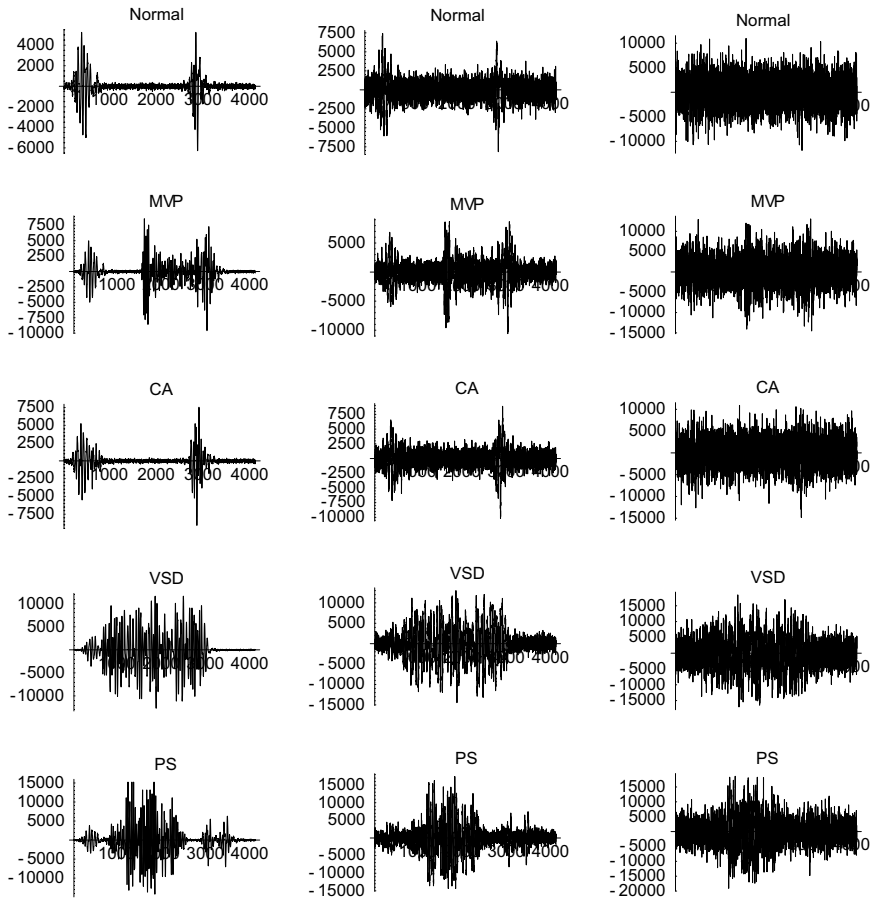

Fig. 12. Representative heart sounds (left to right) without added noise, with noise variance 1000, and with noise variance 3000.

for this variation, classification accuracy as a function of signal-to-noise ratio (SNR) is shown in Fig. 15. For an SNR above 31 dB (which is easily obtainable under most practical circumstances) classification accuracy is 100%.

The modeling and signal-processing techniques described above are very general and could be applied to other signal-processing problems with a relatively modest amount of effort.

8. Conclusions and future work

In this paper, we have introduced a model for the generation of heart sounds, and demonstrated its usefulness as a source of relevant features for cardiac diagnosis.

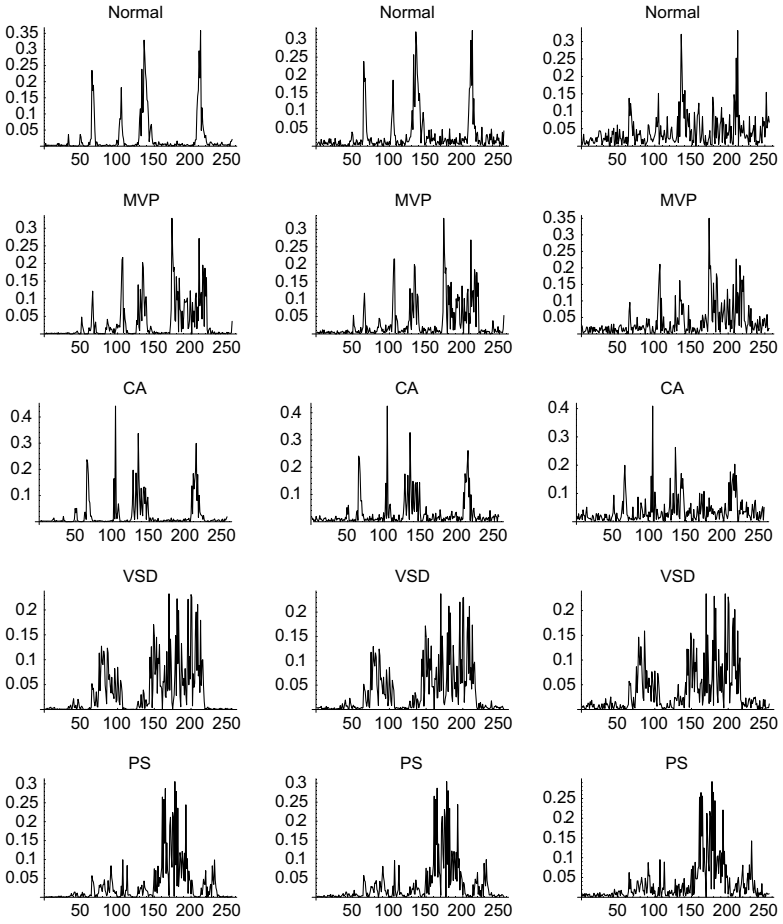

Fig. 13. Feature vectors corresponding to the heart sounds in Fig. 12.

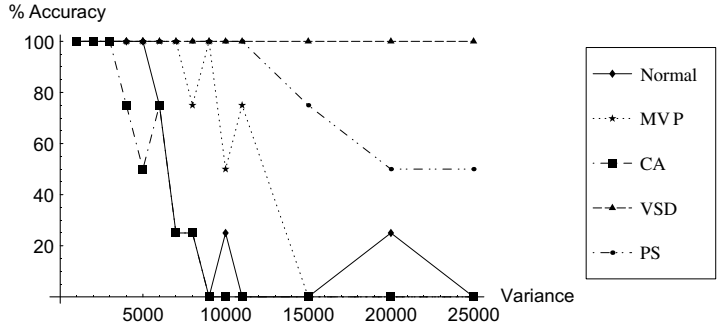

Fig. 14. Classification accuracy (in percent) as a function of the variance of the added noise.

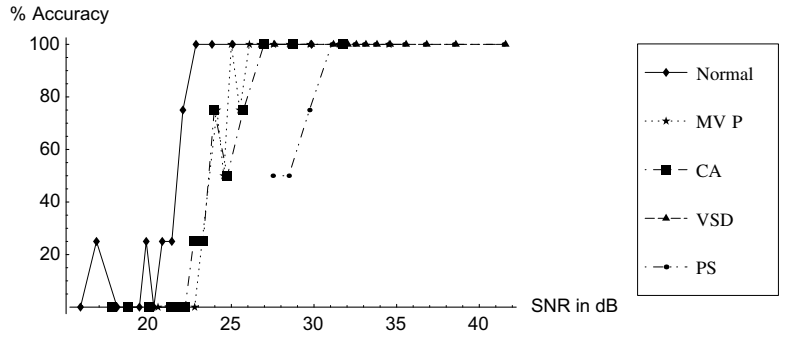

Fig. 15. Classification accuracy as a function of signal-to-noise ratio (in dB).

Establishing a correlation between different pathologies and specific features in the transfer functions, and the evaluation of the utility of this approach as part of a complete computer-based diagnostic aid (e.g., in conjunction with the system described in [16]) are areas of future work.

We have also presented a preliminary study of an approach to machine-aided cardiac diagnosis. The results of this study are promising, suggesting that a system based on this approach will be both accurate and robust, while remaining simple enough to be implemented at low cost.

Areas for future work include the addition of a segmentation component for the automatic extraction of individual heartbeats, the further development of the system to encompass a broader range of symptoms and pathologies, the addition of a knowledge-based component to resolve cases with missing or conflicting symptoms, and an evaluation of the resulting system using a larger and more diverse set of clinical data.

Acknowledgements

This work was supported in part by the Programming Environments Laboratory, Department of Computer and Information Science, Linköping University, Sweden, and by the United States National Science Foundation under grant # 9870454. The authors wish to thank Dr. D. Roy and Dr. C.B. Mahnke for their comments.

Appendix A. Glossary of medical terms

Atrium (pl. atria) the upper two chambers of the heart (left and right).
Aorta the main artery leading from the left ventricle of the heart to the body, providing oxygenated blood throughout.
Aortic valve the heart valve between the left ventricle and the aorta.
Auscultation listening to sounds produced by the body, usually with a stethoscope.

Coarctation of the aorta (CA) a congenital heart defect where a constriction is present in the aorta, restricting the flow of oxygenated blood from the heart to the body. Auscultatory findings include an increased A_2, a systolic ejection murmur, and possibly a systolic ejection click.

Click the term for an abnormal sound associated with valve opening. The most common one is a systolic ejection click which occurs between S_1 and S_2.

Diastole the second phase of the heart cycle starting when the aortic and pulmonary valves close, and ending when the mitral and tricuspid valves close.

Electrocardiogram (ECG) the measurement and recording of electrical signals in the heart. The primary features of a normal ECG are peaks and low points that appear at the same position during systole and diastole. The largest feature—QRS complex, appears at the beginning of diastole, Q is the low point prior to peak, R is the peak and S is the low point after peak.

Hypertrophy thickening of a (heart chamber's) muscle, usually a ventricle, in response to increased workload/pressure to make blood flow.

Mitral valve the heart valve between the left atrium and the left ventricle.

Mitral valve prolapse (MVP) a heart defect where the mitral valve leaflets bulge abnormally up into the left atrium, putting strain on the connecting chords and muscles. The valve may not close completely, causing regurgitation or insufficiency (reverse blood flow). Auscultatory characteristics of MVP include a mid-systolic click and a mid- or late-systolic murmur.

Murmur sounds heard during heart auscultation of a longer duration than S_1, S_2, S_3, or S_4. Attributed to increased turbulence in the blood flow. Murmurs can occur during systole or diastole, or continue though both phases. They are characterized by their timing during the heart cycle, loudness, pitch, location where the sound is heard best, and location(s) to which the sound radiates.

Phonocardiogram a recording of the sounds produced during heart auscultation. Digital versions can be obtained with a digital stethoscope.

Pulmonary stenosis (PS) a heart defect where a narrowing occurs at or near the pulmonary valve, thus restricting blood flow from the right ventricle to the lungs. Auscultatory findings typically include a systolic ejection murmur and a soft P_2, sometimes so soft that S_2 appears single.

Pulmonary valve the heart valve between the right ventricle and the pulmonary artery leading to the lungs.

S_1 the "first" heart sound, always present in normal signals, occurring at the start of the systolic phase of the heart cycle, associated with the closing of the mitral and tricuspid valves. The components from the two valves are so close together in time that they are normally heard as one sound. Some diseases change the blood flow resulting in the two components of S_1 being separated enough that they can be heard.

S_2 the "second" heart sound, present in normal signals, occurs at the end of systole and beginning of the diastolic phase of the heart cycle. It is associated with the closing of the aortic and pulmonary valves and is usually

audible as two "beats" very close together (split), which are labeled A_2 and P_2 for the aortic and pulmonary components, respectively.

S_3 the "third" heart sound, present in about half of normal children, appears in early diastole as rapid filling changes to slow filling of the heart.

S_4 the "fourth" heart sound, not usually audible, appears late during diastole with the P wave of the electrocardiogram, as atrial contraction starts, and shortly before S_1 appears.

Snap an abnormal heart sound associated with the opening of a valve. If present, a snap usually occurs with the opening of the mitral and tricuspid valves between S_2 and S_3.

Systole the first part of the heart cycle starting when the mitral and tricuspid valves close and at the R point in the QRS peak in the ECG. Systole ends when the aortic and pulmonary valves close and diastole starts.

Tricuspid valve the heart valve between the right atrium and right ventricle, which has three leaves (cusps).

Ventricle lower two chambers of the heart (left and right).

Ventricular septal defect (VSD) a congenital heart defect in which there is a hole in the septum between the left and right ventricles (lower chambers) of the heart. This allows oxygenated (left ventricle) and nonoxygenated (right ventricle) blood to mix. Auscultatory findings of VSD typically include a loud pansystolic murmur and an increased P_2. A mid-diastolic murmur may also be present.

References

[1] D. Roy, J. Sargeant, J. Gray, B.H. Adn, M. Allen, M. Fleming, Helping family physicians improve their cardiac auscultation skills with an interactive cd-rom, Journal of Continuing Education in the Health Professions 22 (2002) 152–159.

[2] D.L. Roy, The paediatrician and cardiac auscultation, Paediatric Child Health 8 (9) (2003) 561–563.

[3] C.B. Mahnke, A. Norwalk, D. Hofkosh, J. Zuberbuhler, Y.M. Law, Comparison of two educational interventions on pediatric resident auscultation skills, Pediatrics, in press.

[4] R.L. Donnerstein, V.S. Thomsen, Hemodynamic and anatomic factors affecting the frequency content of Still 's innocent murmur, The American Journal of Cardiology 74 (1994) 508–510.

[5] D. Barschdor, U. Femmer, E. Trowitzsch, Automatic phonocardiogram signal analysis in infants based on wavelet transforms and artificial neural networks, in: Computers in Cardiology 1995, IEEE, Vienna, Austria, 1995, pp.753–756.

[6] B. El-Asir, L. Khadra, A. Al-Abbasi, M. Mohammed, Time–frequency analysis of heart sounds, in: Proc. of the 1996 IEEE TENCON Conf. on Dig. Sig. Proc. Appl., vol. 2, Perth, WA, Australia, 1996, pp. 553–558.

[7] B. El-Asir, L. Khadra, A. Al-Abbasi, M. Mohammed, Multiresolution analysis of heart sounds, in: Proc. of the Third IEEE Int'l Conf. on Elec., Circ., and Sys., vol. 2, Rodos, Greece, 1996, pp. 1084–1087.

[8] J. Ritola, S. Lukkarinen, Comparison of time–frequency distributions in the heart sound analysis, Medical and Biological Engineering and Computing 34 (Supplement 1) (1996) 89–90, Part 1.

[9] H. Shino, H. Yoshida, K.Yana, K. Harada, J. Sudoh, E. Harasawa, Detection and classification of systolic murmur for phonocardiogram screening, in: Proc. of the 18th Int 'l Conf. of the IEEE Eng. in Med. and Biol. Soc.,vol. 1, Amsterdam, The Netherlands, 1996, pp. 123–124.

[10] H. Shino, H. Yoshida, H. Mizuta, K. Yana, Phonocardiogram classification using time–frequency representation, in: Proc. of the 19th Int'l Conf. of the IEEE Eng. in Med. and Biol. Soc., vol. 4, Chicago, IL, 1997, pp. 1636–1637.
[11] S. Rajan, R. Doraiswami, R. Stevenson, R. Watrous, Wavelet based bank of correlators approach for phonocardiogram signal classification, in: Proc. of the IEEE-SP Int'l Symp. on Time–Frequency and Time-Scale Analysis, Pittsburgh, PA, 1998, pp. 77–80.
[12] P. Zhou, Z. Wang, A computer location algorithm for ECG,PCG and CAP, in: Proc. of the 20th Int'l Conf. of the IEEE Eng. in Med. and Biol. Soc., vol. 1, Hong Kong, China, 1998, pp. 220–222.
[13] J.-J. Lee, S.-M. Lee, I.-Y. Kim, H.-K. Min, S.-H. Hong, Comparison between short time Fourier and wavelet transform for feature extraction of heart sound, in: Proc. of IEEE TENCON 99, vol. 2, Cheju Island, South Korea, 1999, pp. 1547–1550.
[14] L.-G. Durand, P. Pibarot, Digital signal processing of the phonocardiogram: review of the most recent advancements, Critical Reviews in Biomedical Engineering 23 (3/4) (1995) 163–219.
[15] J. Verburg, Transmission of vibrations of the heart to the chestwall, Adv. Cardiovasc. Phys. 5 (1983) 84.
[16] N.E. Reed, M. Gini, P.E. Johnson, J.H. Moller, Diagnosing congenital heart defects using the Fallot computational model, Artificial Intelligence in Medicine 10 (1) (1997) 25–40.
[17] J.H. Moller, Essentials of Pediatric Cardiology, second ed., F.A. Davis Company, 1978.
[18] J.A. Shaver, J.J. Leonard, D.F. Leon, Examination of the Heart, Part 4, Auscultation of the Heart, American Heart Association, 1990.